



UNIVERSITÀ DEGLI STUDI DI PADOVA

DIPARTIMENTO DI FISICA E ASTRONOMIA

Corso di Laurea in Astronomia

**THE MAIN SEQUENCE OF THE
STAR FORMING GALAXIES**



Laureando

Sandra Genoveva Castiblanco García

Relatore

Prof. Giulia Rodighiero

Co-relatore

Dr. Chiara Mancini

ANNO ACCADEMICO 2016/2017

Contents

1	Introduction	3
1.1	Estimating the stellar mass of galaxies	5
1.2	The Star Formation Rate	9
2	The Main Sequence of the Star Forming Galaxies (<i>The MS of SFG</i>)	11
2.1	Introduction	11
2.1.1	The location of galaxies in the $(\log M_*, \log SFR)$ plane	11
2.2	The free parameters of the <i>MS of SFG</i>	14
2.2.1	The controversial MS slope (α)	14
2.2.2	The normalisation $\beta(z)$	16
2.2.3	The Scatter	19
3	Conclusions: Implications of the existence of the MS of SFG	21
	Bibliography	24

Chapter 1

Introduction

In the local Universe we observe a wide variety of galaxy types displaying a broad range of structures, sizes and luminosities. Explaining how galaxies were formed and evolved across the history of the Universe is one of the main aims of observational cosmology and answering to this fundamental question is not an easy task. Galaxies are the main blocks of our present Universe and knowing how they assembled and evolved in time will give us important clues about the evolution of the Universe as a whole.

Observations with increasingly accurate instruments (from photography to the modern CCDs) have allowed us to classify galaxies based on their morphological and physical properties. As firstly argued by Hubble (1926), galaxies can be classified in two main morphological types: ellipticals (or spheroids) and spirals, with a further division of spirals into those with bars and those without bars (see Fig. 1.1). Moreover, in the local Universe, there is a well known correlation between colour and morphology. In fact, spheroids are predominantly red in colour due to the fact that they have a very old stellar population and little ongoing star formation, while spirals, usually characterised by being younger and star forming galaxies are blue. Nevertheless, at higher redshifts the case is more complicated.

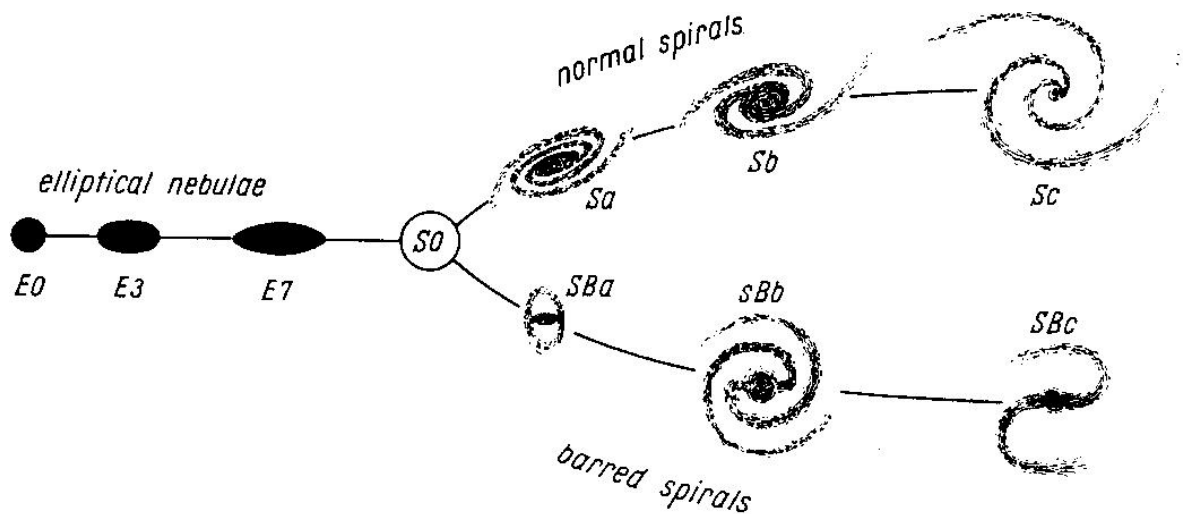


Figure 1.1: The Hubble sequence of galaxies as presented in *The Realm of the Nebulae* Hubble (1936)

Is there an evolutionary link between various morphological classes of galaxies? If yes, what are the processes that lead to morphological mutations in galaxies and how they influence their evolution? What is the role of interactions in the evolution history of galaxies? Which phenomena conspire to shut down star formation in galaxies?

These and many other questions arise from only looking at galaxies in our local Universe, and many efforts have been made in the attempt to find the answers, from both the theoretical and the observational side. In fact, galaxies are mostly made up of not visible cold dark matter which interacts only through gravitational forces and creates the potential well in which ordinary matter (baryons, i.e. the elements we are familiar with) in gaseous form condenses and collapses to form stars. This baryonic matter is only a minority percentage in the mass budget of a galaxy in form of dust, stars, gas, and planets. Nevertheless, modelling its physics is extremely hard as baryons experience a series of complex processes including radiative, mechanical and chemical interactions. Those phenomena involve very different amounts of energy so that we need observations across the whole electromagnetic spectrum to study them. Observations of either individual galaxies, as well as large statistical samples in a wide range of wavelengths, are crucial to improve our understanding of galaxy evolution and are important benchmarks to test the predictions of theoretical models, which still fail to describe the precise physics regulating the star formation and mass assembly in galaxies.

As a result of this necessity, in the past fifteen years many multi-wavelength *deep surveys* have been undertaken, improving our knowledge about the properties of galaxies not only in the local Universe, but also the intermediate and high redshift, so probing the Universe in its earlier epochs. Astronomical surveys allow us to map the sky in different bands and usually are focused on answering specific astrophysical questions. Many of those are indeed focused on the evolution of galaxies and the processes of star formation within them. Such surveys target given areas of the sky with the best available ground based (e.g. VLT, Subaru, Keck, CFHT, ALMA, etc.) and space telescopes (HST, HERSHEL, Spitzer, Chandra, etc.) and instruments, sensitive to one or more specific photometric or spectroscopic frequency. Deep multi-wavelength surveys make possible the study of the same systems in various bands of the electromagnetic spectrum, which greatly improves the accuracy of the analysis. This gives us as well the possibility of testing different diagnostic methods used to estimate galaxy properties, by comparing results in different bands. An example of this kind of deep surveys is the Cosmic Evolution Survey (COSMOS) Laigle et al. (2016), designed to probe the formation and evolution of galaxies as a function of both cosmic time (redshift) and the local galaxy environment. The survey covers a 2 square degree equatorial field with high resolution imaging FROM THE *Hubble Space Telescope* (HST), as well as from X-ray to radio wavelengths, and includes a large amount of spectroscopic data. Over 2 million galaxies are detected, spanning 75% of the age of the Universe. Other important surveys that are worth to mention are SDSS York et al. (2000) (for the local universe), CANDELS Santini et al. (2015), AEGIS Davis et al. (2007) and GOODS Bauer et al. (2011) (for high redshift studies).

Fundamental quantities like the stellar mass (M_*) and star formation rate (SFR) of galaxies are now measured extensively by multi-wavelength surveys taking steps towards our understanding of galaxy evolution and providing new challenges for theoretical models.

For instance, until recently, the high star formation rates and the ensuing stellar mass growth of massive galaxies at early cosmic epochs was widely attributed to violent major mergers. Nevertheless, a number of recent observational findings, based on large samples of galaxies are changing our view of star formation in galaxies. The main and outstanding result of those studies is the existence of a linear correlation between SFR and M_* in logarithmic scale, with a very small scatter since the majority of star forming galaxies (SFGs) follow such correlation at all redshifts, in the literature it is referred to as the Main Sequence (MS) of SFGs (Noeske et al., 2007b).

The aim of this thesis is to make a brief summary of the recent literature about the MS of SFGs, highlighting the important implications it has in our understanding of how galaxies assembled their mass across the cosmic epochs. To this purpose, I will illustrate the most important results, and discuss the main questions still open to debate.

To study and analyse the features of the MS of SFG it is necessary to understand how the SFR and M_* are estimated, therefore the following sections of Chapter 1 briefly describe such methods. The central topic of this work is treated on Chapter 2 where the Main Sequence is described, and the locus of the correlation and its free parameters are treated. Finally on Chapter 3 I discuss the main implications of the existence of the main sequence, and presents the summary and conclusions.

1.1 Estimating the stellar mass of galaxies

The stellar mass of a galaxy is not a directly observable quantity and, therefore, it needs to be estimated from observational data, namely the combined light emitted by all the stars in the galaxy. The most popular technique to convert galaxy light into stellar mass uses Stellar Population Synthesis models to reproduce the observed spectral energy distribution (SED) of the galaxy. It relies only on photometric data, mainly rest frame optical and NIR bands, as the bulk of the M_* is contributed by intermediate-low mass stars with the emission peak at $\sim 1.6\mu m$. Nowadays, this is a standard method for estimating galaxy properties, and large samples of galaxies have been studied with modern broadband photometric surveys (see e.g. SEDS Ashby et al. (2013), CANDELS Santini et al. (2015), COSMOS Laigle et al. (2016)).

To derive a template Spectral Energy Distribution (SED), simulations start by building up a Single Stellar Population (SSP), which is the spectrum of a group of stars originated in a single burst of star formation with a common age and metallicity. The evolution in time of an SSP spectrum is obtained by adding the evolution of the single spectra of stars, given by stellar evolution theory and spectral libraries as a function of their mass and metallicity. This integration is weighted by the Initial Mass Function (IMF), which gives the starting distribution in mass of the stellar population.

A Composite Stellar Population (CSP) is then built by adding the spectra of two or more SSPs of different ages. In this step of the process the ages of the SSPs that contribute to the total M_* of the galaxy at a given time, are regulated by the choice of a Star Formation

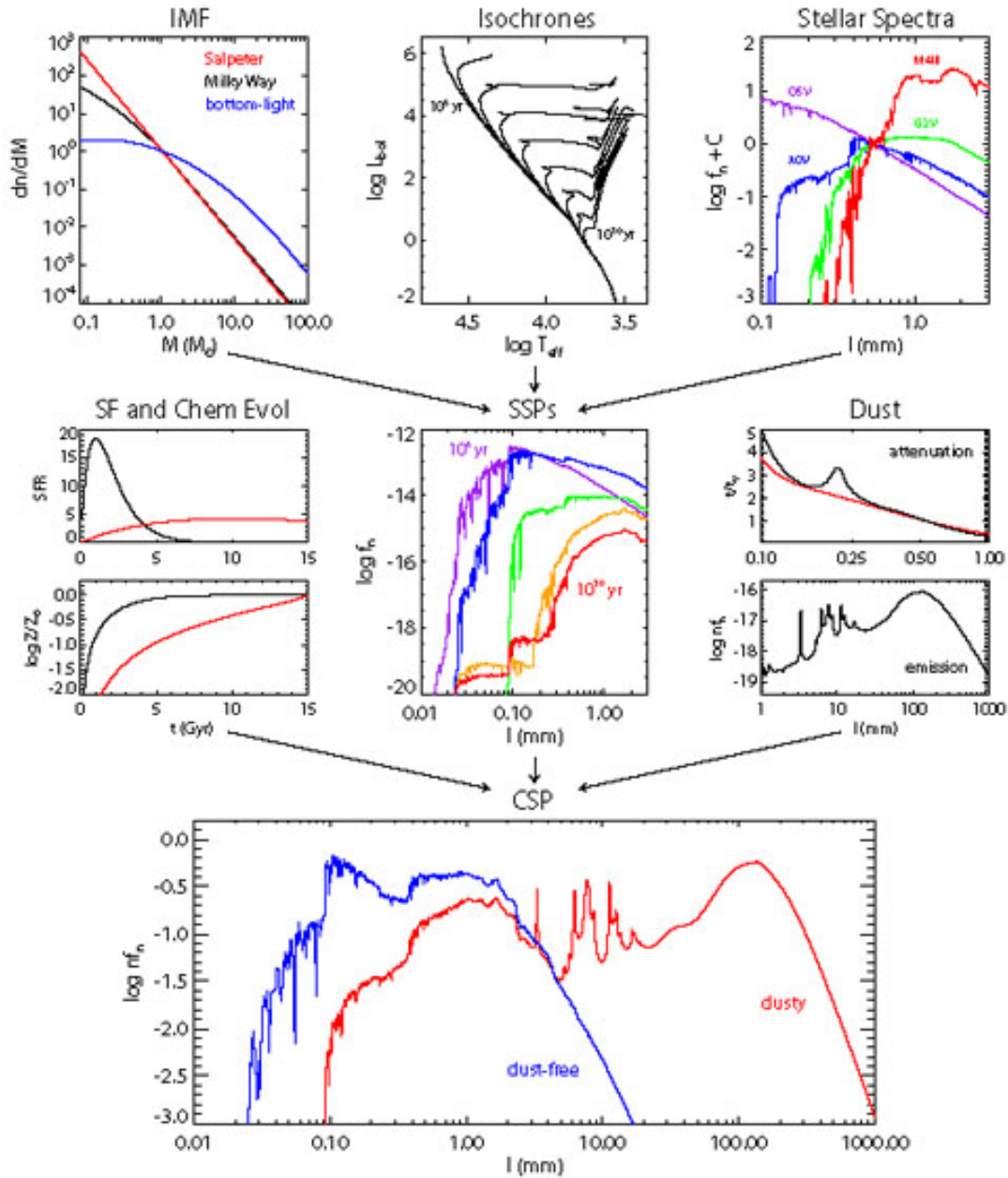


Figure 1.2: Overview of the stellar population synthesis technique. The upper panels highlight the ingredients necessary for constructing simple stellar populations (SSPs): an IMF, isochrones for a range of ages and metallicities, and stellar spectra spanning a range of T_{eff} , L_{bol} , and metallicity. The middle panels highlight the ingredients necessary for constructing composite stellar populations (CSPs): star formation histories and chemical evolution, SSPs, and a model for dust attenuation and emission. The bottom row shows the final CSPs both before and after a dust model is applied. From Conroy (2013)

History (SFH), which gives the evolution with time of the star formation rate. Finally, the effect of dust in the interstellar medium needs to be included in the form of an attenuation law. see fig. 1.2.

Therefore, one can reproduce the galaxy spectrum by fitting the multi-band photometric data-points with the spectral templates aforementioned. Given the galaxy redshift, either spectroscopic or photometric, the best fit SED model is chosen among the available templates, by minimising the χ^2 between the observed and modelled fluxes. The final best fit result will be sensitive to a large set of variables, such as the choice of stellar population models and IMF, the metallicity, the amount of dust and the used extinction law (e.g. (Calzetti et al., 2000; Allen, 1976; Seaton, 1979; Fitzpatrick, 1986; Prevot et al., 1984))

Finally, the stellar mass is obtained from the Mass-to-light ratio (M/L) of the best fit SED and hence it strongly depends on the redshift, age and SFH of the model. In this step, the redshift information is set as an input parameter, in order to minimise the number of free parameters and produce reliable results for the galaxy stellar mass. The most used IMF in the literature are the Salpeter (1955); Chabrier (2003); Kroupa (2001), IMFs. The impact of Kroupa and Chabrier IMFs is similar in the resulting values of mass, while Salpeter IMF is observed to produce masses larger by a factor between ~ 1.7 and 2 with respect to the others. In terms of the reddening law, the most used in recent literature is the Calzetti et al. (2000). The SFH is the most uncertain parameter in the SED-fitting and, as a consequence, it produces an uncertainty in the computation of M_* . Another important source of uncertainty is the quality of the photometry and its wavelength coverage. Particularly important for an accurate estimate of the stellar mass is the inclusion of rest frame NIR data in the fit, as mentioned before the intermediate-low mass stars make up the bulk of the galaxy M_* and have the peak of emission in the NIR so that including these bands in the SED-fitting is crucial for a proper derivation of M_* . Uncertainties are usually estimated applying the codes to mock catalogues, for example Mobasher et al. (2015) found that a typical uncertainty in M_* estimates is $\sim 0.2dex$.

The following two figures show the results for SED fittings of galaxies at different redshift.

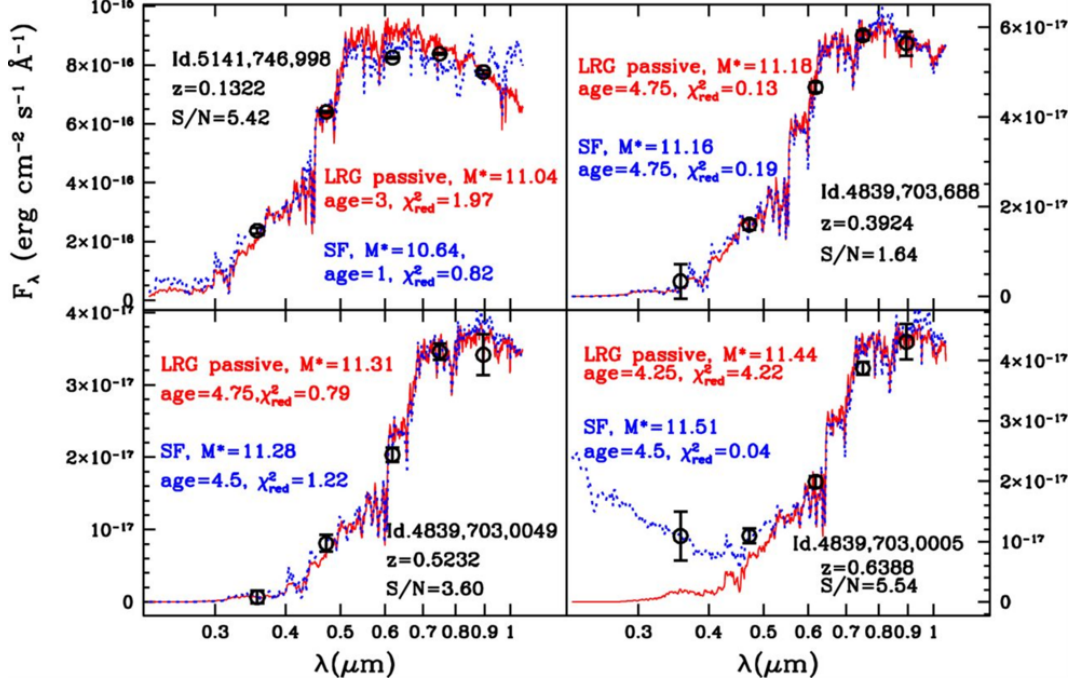


Figure 1.3: Examples of SED-fit results for four BOSS galaxies, in order of increasing spectroscopic redshifts from top left to bottom right. The red and blue lines display the best-fitting models and labels show $\log M_*/M_\odot$, age (Gyr), reduced χ^2 , as obtained using the LRG-passive and the star-forming (SF) templates, respectively. Spectroscopic redshifts and median photometric S/N are indicated. From Maraston et al. (2013)

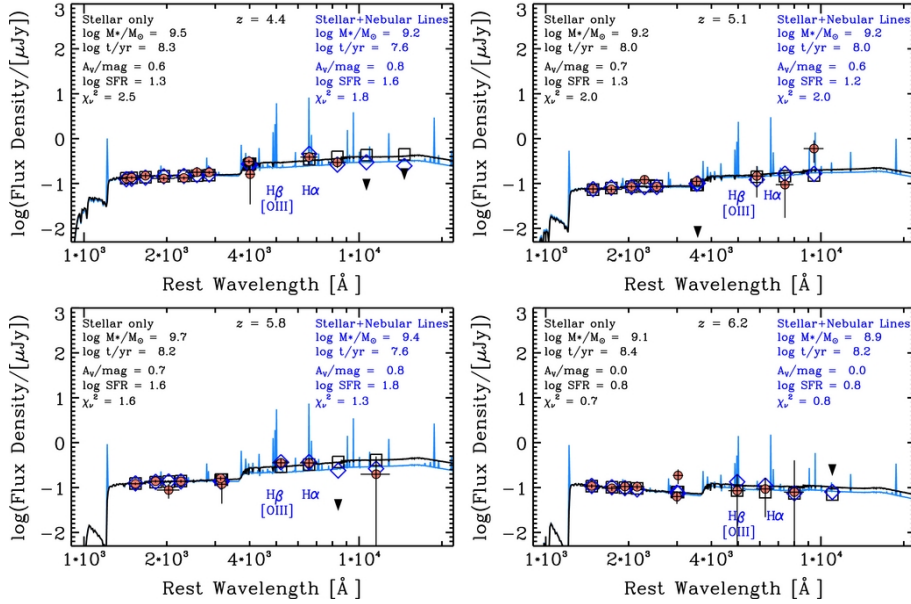


Figure 1.4: Four example galaxies from a sample with SED fits that do include nebular emission lines (blue curves) and do not include emission lines (black curves). Circles are the observed photometry and diamonds (squares) are the fluxes of the best-fit SED with (without) emission lines. All objects were fit assuming a constant star formation history and starburst-like dust-attenuation. From Salmon et al. (2015).

1.2 The Star Formation Rate

The star formation rate is the total mass of stars formed per year, often given as solar masses per year. The usual way to estimate such a rate is to derive it from monochromatic or integrated luminosity measured at wavelengths that are characteristic of young stellar populations. The aim is to sample the youngest stars avoiding as much as possible any old population or contributions from other sources in the galaxy. Each selected band or wavelength probes a slightly different population, and therefore a different time scale, for example H_α emission is produced by recombination in HII regions that have been photoionized by early-type stars with lifetimes $< 20 Myr$, while the UV continuum comes from a wider range of massive stars with longer lifetimes ($\sim 10^8 yr$).

SFR indicators cover a wide range of bands and monochromatic wavelengths from the X rays, to the radio and for each of them a relation between the SFR and the measured luminosity has been calibrated, assuming an IMF and an appropriate SFH. In fact, most synthesis models provide relations between the SFR per unit mass or luminosity and the integrated colour of the population. In what follows I will describe the most common tracers of SFR, mentioning the time scales they sample and the sources of uncertainty in each case.

- **The Ultraviolet** $\sim (1500 - 2800) \text{ \AA}$

This is the natural direct tracer of SFR as the youngest and most massive stars ($> 5M_\odot$) have their peak of emission in the ultraviolet. It is usually considered that the SFR remains constant over time-scales bigger than the life times of these stars. Consequently, UV emission, ideally at $\lambda \in (1250 - 2500) \text{ \AA}$ Kennicutt (1998), traces stars formed over the past $10 - 200 Myr$ and it is proportional to the SFR, where the proportionality constant depends on the IMF. The most significant uncertainties in this diagnostic lie in the needed corrections for dust attenuation and the dependence on the IMF. Other less significant uncertainties are carried by the absorption of UV light due to the metal content in the galaxy or the UV emission by an AGN.

The highest advantage of this tracer is that it relies only on photometric data, which is widely available in a broad range of redshifts, allowing us to probe distant star forming galaxies.

- **The Optical and NIR** (or recombination and forbidden lines)

In the ISM only stars with masses $> 10M_\odot$ and lifetimes $< 20 Myr$ contribute significantly to photoionize the gas, therefore the emission lines produced by the recombination processes are an instantaneous measure of a galaxy's SFR (e.g. H_α , H_β , P_α or forbidden lines: O[II] and O[III]). The most widely used is H_α .

Calibrations of the SFR from these lines are made using evolutionary synthesis models. These indicators rely on the assumption that the bulk of massive star formation is traced by the ionized gas and therefore uncertainties arise from the chosen IMF and its slope at the higher stellar masses. Additionally, these lines are affected by dust extinction, and in the case of the forbidden lines, metallicity can as well affect the derived SFR.

- **The MID and Far Infrared**

Optical and UV light produced by young stellar populations heats up the dust in the ISM which in turns re-radiate such energy in the FIR wavelengths, making such band a suitable tracer for SFRs. One of the advantages of this indicator is that it can be used to complement the UV light as SFR indicator, as it accounts for the extinguished high energy photons. As IR emission traces indirectly the UV light, the estimated SFRs are sensitive to the same $\sim 100Myr$ timescales. Uncertainties in these estimations arise from the difficulty in excluding evolved populations, in fact faint UV light produced by old low-mass stars is as well absorbed and re-emitted by the dust with a peak in $\lambda \in (100 - 150)\mu m$, additionally the presence of AGNs emissions can as well heat the dust. Most of the available calibrations use the integrated luminosity over the full mid and far IR spectrum, $(8 - 1000)\mu m$ and are derived using synthesis models, which are affected by the chosen IMF and SFH.

- **The radio**

Synchrotron radio emission at 1.4GHz due to relativistic electrons from recent supernovae explosions is a good SF tracer as it is not affected by dust. Assuming that the correlation between the 1.4GHz radio frequencies and the total luminosity in the IR in the local Universe still holds at high redshifts, this tracer is an indirect measure of the bolometric IR luminosity and therefore is sensitive to similar timescales $\sim 100Myr$.

Combinations of these tracers in multi-wavelength surveys improve the accuracy of the SFR estimations, e.g. by adding the SFR obtained from total IR luminosity to that obtained from rest frame UV uncorrected by reddening, in order to estimate obscured and unobscured star formation (Daddi et al., 2007), or combining H_α emission lines and luminosity at $24\mu m$ to derived SFR corrected by dust attenuation (Kennicutt et al., 2009).

Chapter 2

The Main Sequence of the Star Forming Galaxies (*The MS of SFG*)

2.1 Introduction

The existence of a correlation between the stellar mass and SFR in galaxies has already been introduced in Chapter 1. This relation is sometimes referred to as the Main Sequence of star-forming galaxies (hereafter the MS of SFG), the term coined by Noeske et al. (2007a) in order to suggest an analogy with the well known stellar main sequence. Today, ten years later, the term is still in use, although the validity of the analogy is not yet complete and questions about this MS of SFG being a paradigm of galaxy evolution (as it is the case for the stellar main sequence) persist, (see for example Eales et al. (2017, 2018); Feldmann (2017)). Nevertheless, the MS of SFG has allowed the scientific community to suggest some possible tracks of galaxy evolution and stellar mass assembly, which I will describe briefly in chapter 3.

The following are some of the analogies with the stellar main sequence that have a notable consensus:

1. Galaxies spend most of their life (in the sense of active star formation) in the so called galactic main sequence, analogous to the fact that stars spend most of their life in the stellar main sequence.
2. Massive Galaxies become passive faster than low mass ones similar to the fact that massive stars have shorter lives.
3. Most galaxies seem to go through a short luminous starburst phase, which can be paralleled with the bright phase of giants and AGB stars. In this case, such phase could actually be the transition step to become quenched galaxies, as in the case of stars becoming much more luminous before dying.

2.1.1 The location of galaxies in the $(\log M_*, \log SFR)$ plane

Results from different surveys studying samples of galaxies at a given z show that in the plane (M_*, SFR) , it is possible to clearly identify three different populations. The main

group is formed by the majority of star forming galaxies defining the tight main sequence, object of this thesis. The second group is located above the MS, and it is evidently less populated. These galaxies are called Starbursts because they have much higher SFRs than those of “normal” star forming galaxies with the same mass sitting along the MS. This clear division of the star forming galaxies is interpreted as the “bimodality of star formation” (Guo et al., 2013), suggesting that there are two modes that control the growth of a galaxy’s stellar mass: a normal mode characterised by a relatively steady rate which defines the MS and a highly efficient mode generally interpreted as starburst driven by mergers. Finally, the third group is formed by those systems scattered below the SF MS, the passive or quenched galaxies that are characterised by very low or none SFRs compared with the SFR values of the MS galaxies at the same masses.

The first studies that argued the existence of the MS were Brinchmann et al. (2004); Noeske et al. (2007a); Elbaz et al. (2007); Daddi et al. (2007) in the local Universe ($z < 0.2$); and at intermediate redshifts ($0.5 < z < 3$), since then many others have followed confirming the existence of the MS up to redshift ~ 6 (Whitaker et al., 2012; Salmon et al., 2015)

In figures 2.2, 2.3, 2.1 I show the MS as obtained by the studies based on the largest samples from some of the most important galaxy surveys (SDSS, CANDELS), both in the local Universe and at high redshift. Fig.2.1, shows a different view of the MS of star forming galaxies. In their paper Renzini and Peng (2015), in an effort to eliminate discrepancies between different studies, proposed a 3D definition of the MS of SFG. This 3D version highlights the main feature of the strip obtained on the SFR , M_* plane. The third-dimension gives (the number of galaxies $\times SFR$), hence showing where most of the star formation takes place. The ridge of the star-forming peak is their adopted definition of the main sequence. The small bump in the east side of the main peak is due to quenched galaxies, some indeed still supporting a low level of star formation.

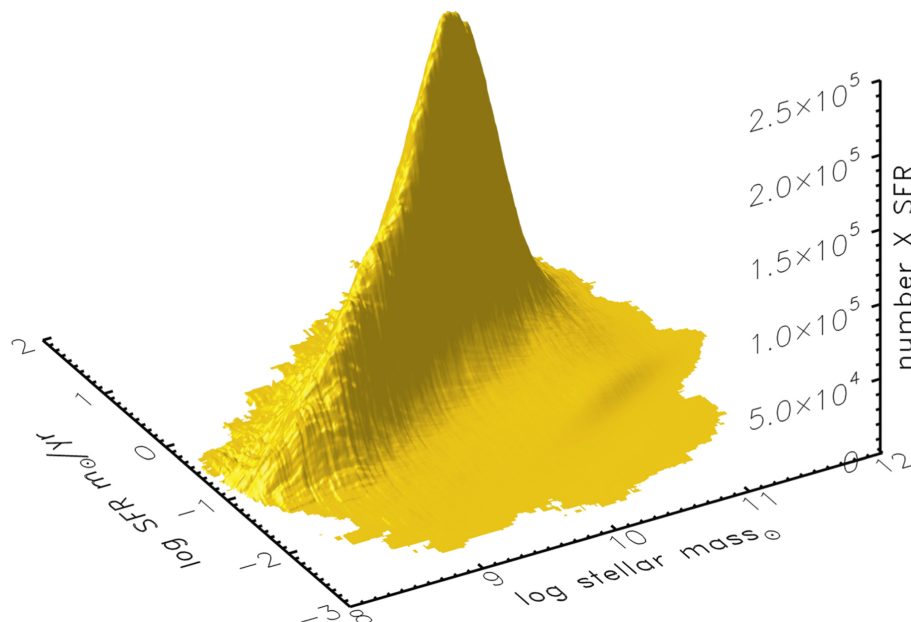


Figure 2.1: Three dimensional SFR, M_* relation for local galaxies in the SDSS database and $0.02 < z < 0.085$. From Renzini and Peng (2015).

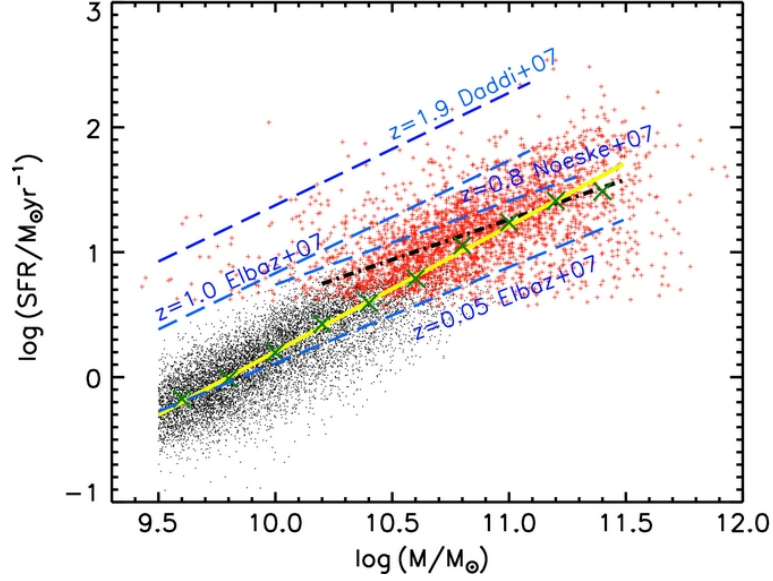


Figure 2.2: SFR, M_* relation for a sample of SFG (red crosses: $24\mu\text{m}$ detected, black dots; $24\mu\text{m}$ undetected). The yellow solid line is the best power-law fit to the relation, suggesting a slope of 1. The best fit to the mean SFRs (green X) also gives the same slope within uncertainties. The MS relations from previous works are also shown for comparison (Noeske et al., 2007b; Elbaz et al., 2007; Daddi et al., 2007). The black dash-dotted line with a slope of 0.64 is the best fit to the $24\mu\text{m}$ detected SFG. Noeske et al. (2007b) gave a shallower slope at the same redshift because of incomplete SFG sample selection. In this case, the slope of the SFR, M_* relation is mostly determined by the dominant population of $24\mu\text{m}$ undetected SFG. From Guo et al. (2013)

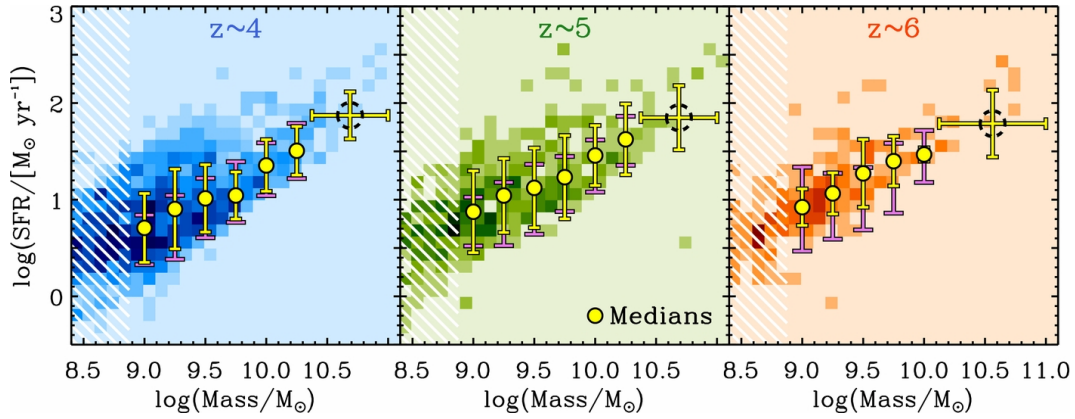


Figure 2.3: SFR, M_* relation for the CANDELS galaxy samples. The darker-shaded regions indicate a higher number of individual objects in bins of stellar mass and SFR. Yellow circles are medians in bins of mass and yellow error bars are their confidence range. The median SFR of a wider, high-mass bin is also shown by the dashed black circle. The white hatched regions mark the limit above which completeness effects become negligible. The authors measure a slope of ~ 0.6 , with no evidence for evolution over the redshift range $z \sim 6$ to $z \sim 4$. From Salmon et al. (2015).

The general agreement is that the main sequence has an analytical expression that in logarithmic scale is given by:

$$\log(SFR) = \alpha(z) \log(M_*) + \beta(z) \quad (2.1)$$

Where α and β are the free parameters of the fit, namely the logarithmic slope and normalisation. In general, the normalisation is well defined and there is wide consensus about its evolution with cosmic time at fixed mass. In fact, it is related to the evolution of the specific SFR defined as:

$$sSFR \equiv \frac{SFR}{M_*} \quad [yr^{-1}] \quad (2.2)$$

which is an increasing function of redshift, due to the presence of a higher content of gas in galaxies at earlier times. Hence, the value of β increases with redshift such as the galaxy average sSFR. see. § 2.2.2.

The observed scatter of the MS is quiet tight and it is measured between ~ 0.2 and ~ 0.3 dex, at all redshifts, which implies that Star Formation in the majority of galaxies, at least up to $z \sim 6$ (the limit of the current available data) is a fairly ordered process happening on long time scales.

In the case of the slope α the consensus is not as wide as that for scatter and sSFR, in fact α varies between 0.6 and 1, in different studies. (Speagle et al., 2014). see §2.2.1

In the following sections of this Chapter I will describe in more detail the parameters of the correlation α and β as well as the scatter of the galaxies along the MS.

2.2 The free parameters of the *MS of SFG*

2.2.1 The controversial MS slope (α)

The importance of α , i.e. the slope of the MS, lies in the fact that it controls the relative growth of high-mass versus low-mass galaxies. Determining whether it evolves with redshift and stellar mass, and the form of such evolution is crucial for our understanding of star formation in galaxies.

As mentioned before, while the existence of the MS is generally undisputed, its slope seem to vary significantly from one observational study to another, with typical values between ~ 0.6 and unity and its value may be a function of redshift as well (Speagle et al., 2014; Pannella et al., 2009; Karim et al., 2011; Whitaker et al., 2012). Such differences rise from factors like the criterion used to select SFG and the adopted SFR and stellar mass diagnostics (Rodighiero et al., 2010, 2014; Speagle et al., 2014; Karim et al., 2011; Guo

et al., 2013). For example Whitaker et al. (2012) found that the evolution with z of the MS slope is given by $\alpha(z) = 0.70 - 0.13z$ from $z \sim 0$ to $z \sim 2.5$ while Karim et al. (2011) found little or none z evolution within the same redshift range.

With regards to the differences in the slope between various studies due to the choice of SFR indicators, one evident example is given by the comparison between UV and IR. In fact Rodighiero et al. (2014) have shown that selecting galaxies in a passband that is directly sensitive to the SFR (such as the rest-frame UV or the FIR) automatically induces a Malmquist bias in favour of low-mass galaxies with above average SFR, thus flattening the resulting $SFR - M_*$ correlation. as seen in fig. 2.4

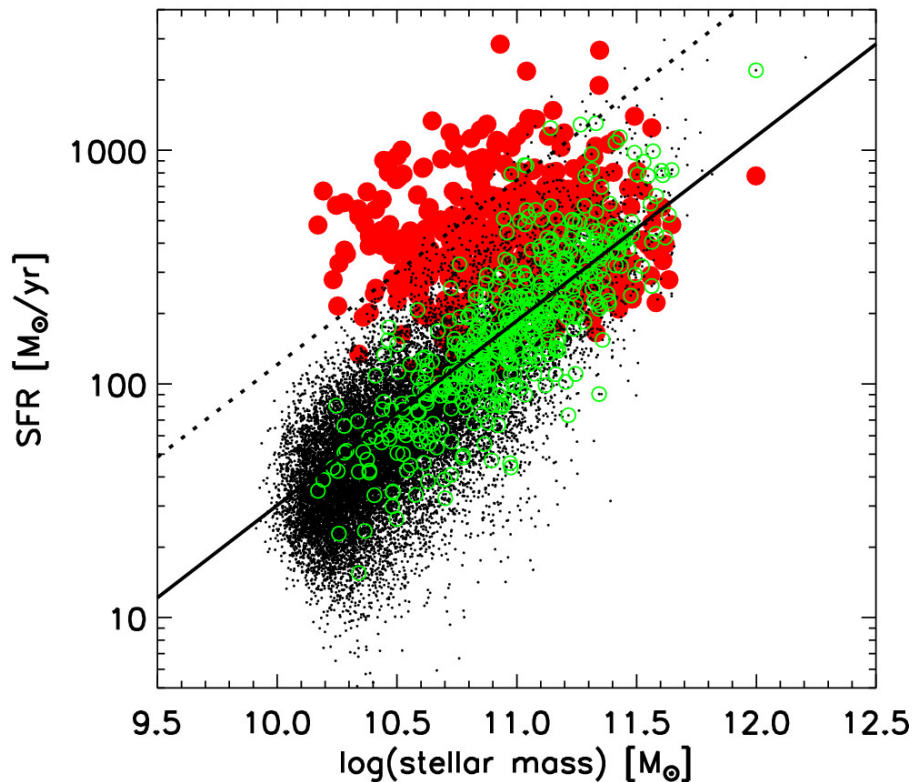


Figure 2.4: The SFR, M_* relation for a star forming colour selected sample, (small black dots), for which both $SFR(UV)$ (green open circles) and $SFR(FIR)$ red dots are reported. The solid line indicates the MS and the dotted line the limit $SFR(UV) = 4 \times SFR(MS)$ relation at $z \sim 2$. From Rodighiero et al. (2014)

Recent studies have also shown that the MS tends to flatten at high stellar masses ($\log(M_*/M_\odot) > 10.5$) a phenomenon called the bending of the MS. The fitted relation in those cases has been suggested to be a double power law, one for the higher masses and another one for the lower masses. One suggested explanation for such change in the slope at high masses is a gradual reduction in the star formation efficiency or slow quenching, due for example to stellar growth of quiescent bulges in star-forming galaxies. (Salmon et al. (2015); Lee et al. (2015); Schreiber et al. (2015) see Fig.2.5).

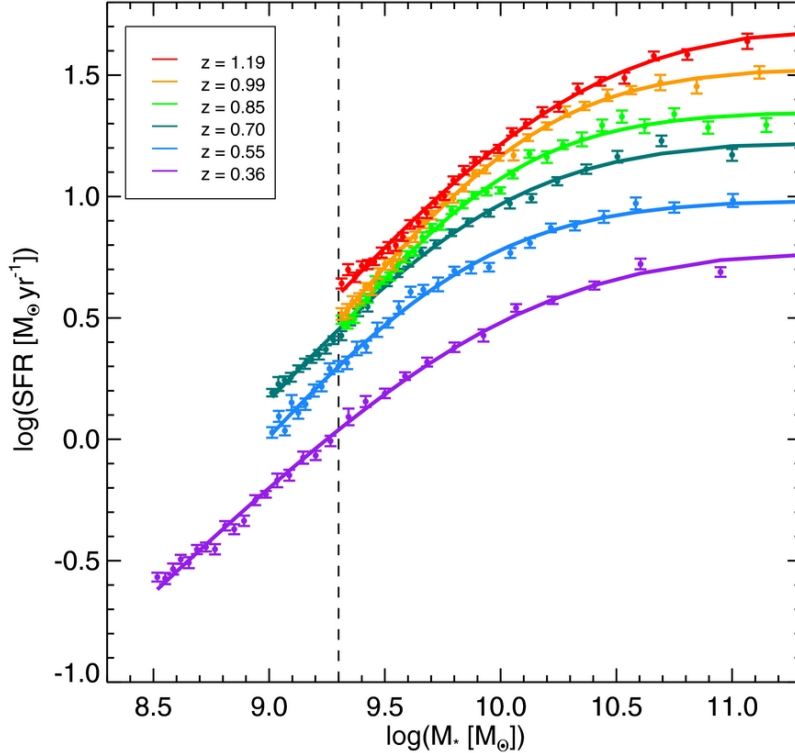


Figure 2.5: Median SFR in six equally populated redshift bins that have been split into 30 equally populated stellar mass bins. Solid lines represent the best-fit curve to the model, given by a double power law. Vertical dashed line represents the stellar mass limit below which photometry has not been well calibrated. From Lee et al. (2015)

2.2.2 The normalisation $\beta(z)$

The normalisation of the MS of SFG, β , as mentioned before, is related to the evolution of the sSFR. In fact for the correlation given in 2.2, β will be defined as:

$$\beta = \log \frac{SFR}{(M_*)^\alpha} \quad (2.3)$$

Therefore for a main sequence characterised by a unity slope, beta and the sSFR would be the same, nevertheless most studies report a slope different than 1. It is important here to understand the physical meaning of the sSFR as defined in Eq. 2.2, it sets a characteristic time-scale of star formation for individual galaxies: the doubling time of the stellar mass of individual galaxies. Sometimes this is interpreted as the present to past average star formation of a galaxy, or birthrate at a given cosmic time, (Brinchmann et al., 2004; Karim et al., 2011; Madau and Dickinson, 2014).

The sSFR is a declining function of cosmic time, in other words, an increasing function of redshift for all stellar masses, confirming that the bulk of star formation happened at earlier epochs. (Noeske et al., 2007a; Rodighiero et al., 2010). Nevertheless, recent studies have found that this decrease becomes less prominent at redshifts higher than

$z = 3$ (see Fig.2.6). Such evolution with redshift for a given stellar mass, seems to have an exponential behaviour from $z \sim 0$ to $z \sim 2$ given by $sSFR = (1 + z)^n$, with $n \in [2.8 - 3.5]$, as seen in fig. 2.6 where the results of different studies up to $z \sim 6$ for a fixed M_* are reported. It is also visible what some studies report as a flattening or slow increasing of the sSFR after $z = 2$. (Daddi et al., 2007; Ilbert et al., 2015; Karim et al., 2011; Sargent et al., 2014). The rapid decline of the sSFR from $z \sim 2$ to $z = 0$ is largely attributed to gas exhaustion (Noeske et al., 2007b).

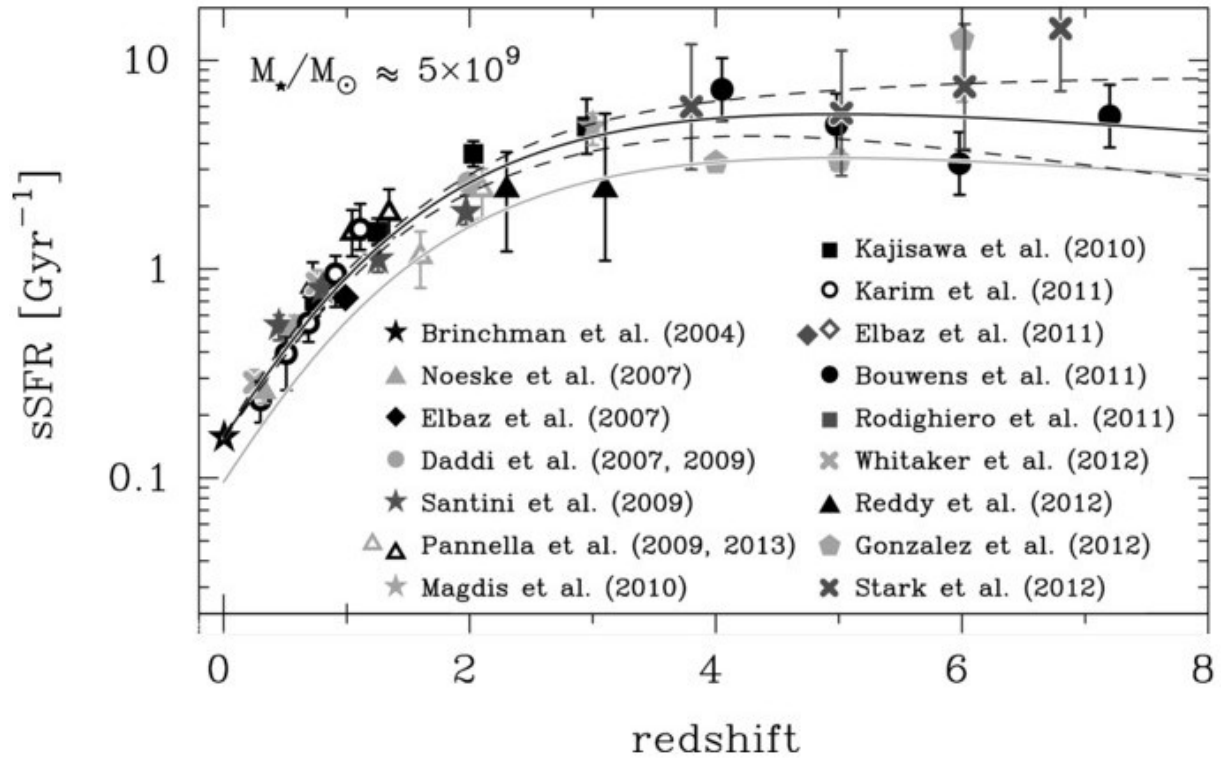


Figure 2.6: Redshift dependence of the sSFR of SFG with stellar mass $M_*/M_\odot \simeq 5 \times 10^9$, as published in the recent literature. Measurements derived based on image-stacking are indicated with open symbols and error bars denote the uncertainty on the sSFR-average rather than the sSFR-scatter in the population. Solid/dashed black lines the best-fit evolution of the sSFR, dot-dashed line evolution according to $(1 + z)^{2.8}$ from Sargent et al. (2014)

Fig. 2.7 also shows that the mean sSFR of star-forming sources rises with redshift, up to a factor ~ 15 for the most massive galaxies ($M_* > 10^{11} M_\odot$), implying that galaxies tend to form their stars more actively at higher redshifts. The mean sSFR seems also to flatten at $z > 1.5$ for ($M_* > 10^{10.5} M_\odot$). Moreover, the most massive galaxies have the lowest sSFR at any redshifts. As shown in this figure, they have already so large stellar masses at $z = 0.7$ to 2.5 that they would require steady SFR at the observed level during the whole Hubble time at that redshift to form. In contrast with the shorter doubling times that lower masses require now a days, this quenching of the star formation supports the so called “downsizing paradigm”, which suggests that the bulk of star formation moves from massive galaxies to less massive ones with time.

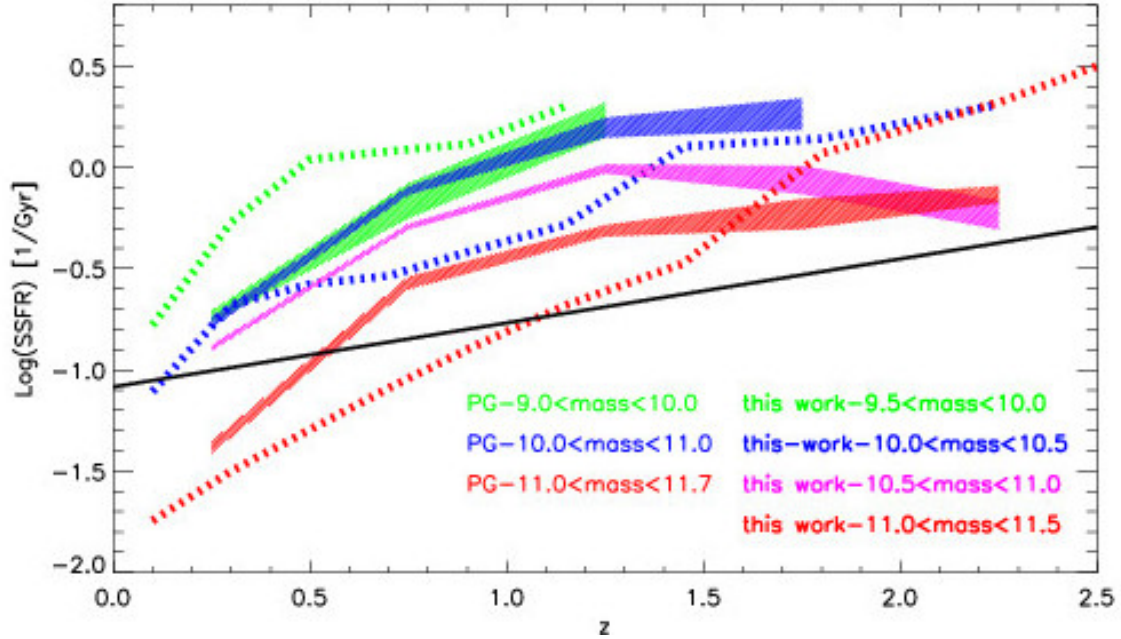


Figure 2.7: sSFR, M_* relation for different mass bins of SFG. The figure shows the results from Rodighiero et al. (2010) (shaded colours) and those from Pérez-González et al. (2008) (dotted lines). Error bars denote the uncertainty on the sSFR-average rather than the sSFR-scatter in the population. Solid/dashed black lines the best-fit evolution of the sSFR, dot-dashed line evolution according to $(1+z)^{2.8}$ from Sargent et al. (2014)

Another interesting feature of the normalisation is the way it evolves decreasing with stellar mass at all epochs, although it seems to be almost flat for masses $M_* < 10^{10} M_\odot$. This is even more evident when only SFG are selected, ie. excluding passive galaxies from the sample (Karim et al., 2011). Nevertheless the majority of the studies that include $z = 2$ redshifts has confirmed that at such redshift the relation is nearly mass independent. (Karim et al., 2011; Rodighiero et al., 2010) see fig. 2.8.

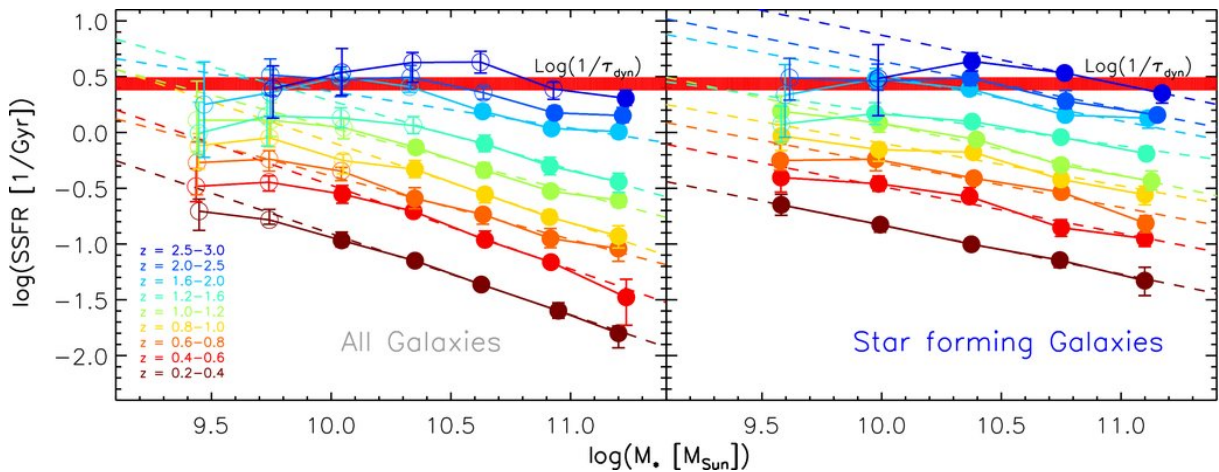


Figure 2.8: Radio-stacking-based measurement of the SSFR as a function of stellar mass at $0.2 < z < 3.0$. From Karim et al. (2011)

2.2.3 The Scatter

One of the impressive consensus among different studies is that the width of the MS strip is relatively small, i.e. the range of SFRs that SFG of the same mass span at a given redshift is contained within a small scatter, generally between ~ 0.2 and $0.3dex$ (Whitaker et al., 2012; Schreiber et al., 2015; Noeske et al., 2007a) among many others. Moreover the scatter seems to be the same at all redshifts. Studies based on large and unbiased samples of star-forming galaxies have also shown that the measured scatter in the MS is mostly caused by intrinsic differences in sSFR, and marginally contributed by observational uncertainties (Salmi et al. 2012). Different sSFR are in turn related to variations in the galaxy star formation history (SFH), which involve gas accretion and physical processes triggering or quenching the star formation (Guo et al. 2013). Hence, the principal implication of the observed small scatter of the correlation $SFR - M_*$ is that star formation in the majority of galaxies, at least up to $z \sim 6$, is a fairly ordered process occurring with long timescales in a quasi steady mode, as opposed to stochastic processes like starbursts, possibly due to mergers.

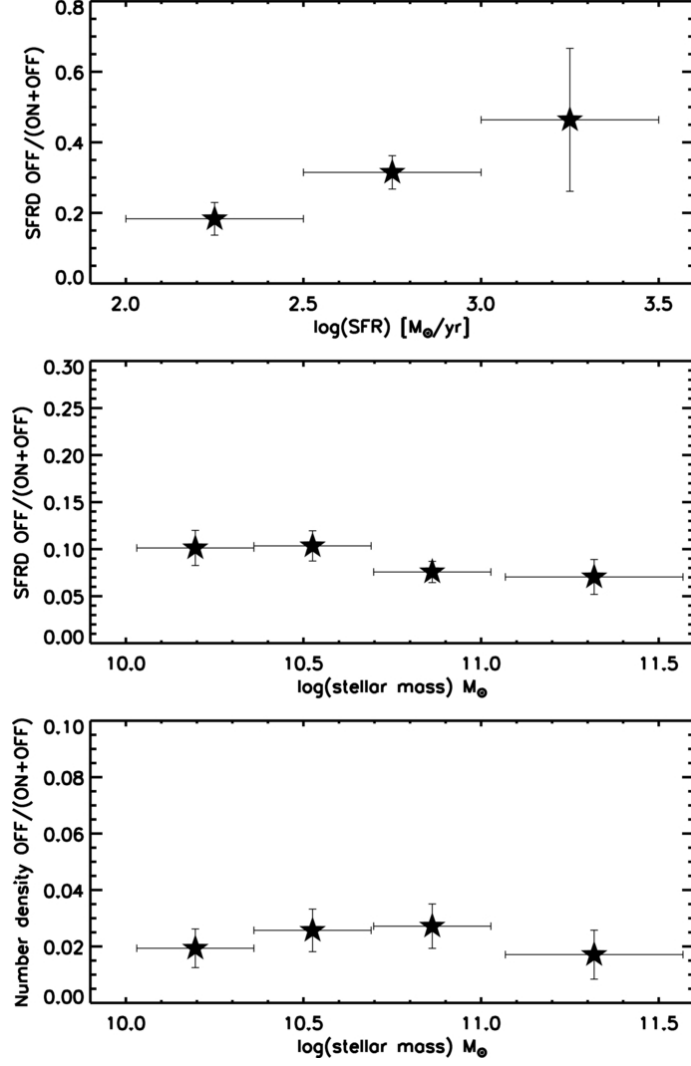


Figure 2.9: Contribution of off-sequence galaxies to the total SFR density in different SFR bins (top panel) and stellar mass bins (middle panel). In the bottom panel we also report the number density percentage of off-sequence sources. Error bars are Poisson. From Rodighiero et al. (2011)

In fact, it has been showed in recent studies that starbursts play a minor role for the formation of stars in galaxies, since they represent only a few percentage of the star forming population and contribute only to $\sim 10 - 15\%$ to the cosmic SFR density of the Universe at all redshifts see fig. 2.9(Rodighiero et al., 2011; Schreiber et al., 2015). These results suggest that two different modes of star formation may be responsible for the growth of stellar mass in galaxies. The first one is a steady and secular mode, present in most star forming galaxies, in which cold gas is provided fuelling constant star formation. The second one less frequent, in which hot gas, most probably provided by mergers, eventually triggers high rates of star formation in short burst episodes.

Chapter 3

Conclusions: Implications of the existence of the MS of SFG

It is clear that huge progress has been made in the last fifteen years in the galaxy star formation and mass assembly history thanks to the availability of the many multi-wavelength surveys. In this thesis I review and describe one of the most relevant results of the last decade in the field of galaxy formation and evolution: the existence of the Main Sequence of the Star Forming Galaxies. Its major role has been to shed light on how star formation proceeds in galaxies over cosmic time. Therefore, as a final conclusion to this review I summarize here the implications of its existence.

One outstanding result of the observations reported in the many studies mentioned in the chapters above is that the Universe at high redshifts (up to $z \sim 6$) is populated by very actively star forming galaxies with SFRs $\geq 100 [M_{\odot}/yr]$ being quiet common. This is a surprising picture when compared with our local Universe, where such high SFRs are characteristic of only a few number of systems called Starburst. Such galaxies in our local Universe, are considered to be in a relatively short and temporary process of enhanced star formation. Therefore the above mentioned observational results seemed to suggest that the majority of star-forming galaxies observed at high z were caught in a transient process, which is very unlikely. The study of the MS of SFG has solved this problem, probing that higher SFRs were the norm in the distant Universe. Nevertheless, starburst galaxies (with SFR ~ 10 times higher than MS galaxies) also exist at high redshift, and it is still unsolved how they take place and evolve and what triggers their star formation, although merger events seem to be the strongest candidate. However, they just represent a small percentage ($\sim 2\%$) of the global star-forming galaxy population, and their contribution to the total star formation rate density (and galaxy mass assembly) is only $\sim 10 - 15\%$ at all redshifts.

The relatively small scatter found in studies about the main sequence, has a profound consequence in the history of star formation in galaxies as it means that the majority of star forming galaxies remain on the main sequence for most of their life, meaning that there is one principal mode of star formation in galaxies. This in conjunction with the fact that the slope of the $\log SFR$ versus $\log M_*$ relation for only star forming galaxies is almost constant over cosmic time, implies that such process is a fairly ordered one taking place during long periods of time i.e. nearly the whole active life of the galaxy.

The evolution of the MS normalisation with redshift for different stellar masses, shows how the bulk of star formation is moving from massive galaxies to lower mass ones. Massive galaxies formed their stars earlier and more rapidly than their low mass counterparts, confirming the “downsizing scenario” proposed by Cowie et al. (1996).

Finally, in the introduction of Chapter 2 I mentioned how the name of the MS of SFGs was chosen as a reminder of the analogy and interesting parallel that may be present between the Stellar Main Sequence and Galaxy evolution on the SFR and M_* plane. In fact the dependence of SFR on stellar mass allows us to imagine that a galaxy can move along the plane as a result of the different physical processes that shape its evolution. Therefore, some tracks have already been proposed for the evolution of galaxies in the (SFR, M_*) plane, as shown in the cartoon in fig. 3.1.

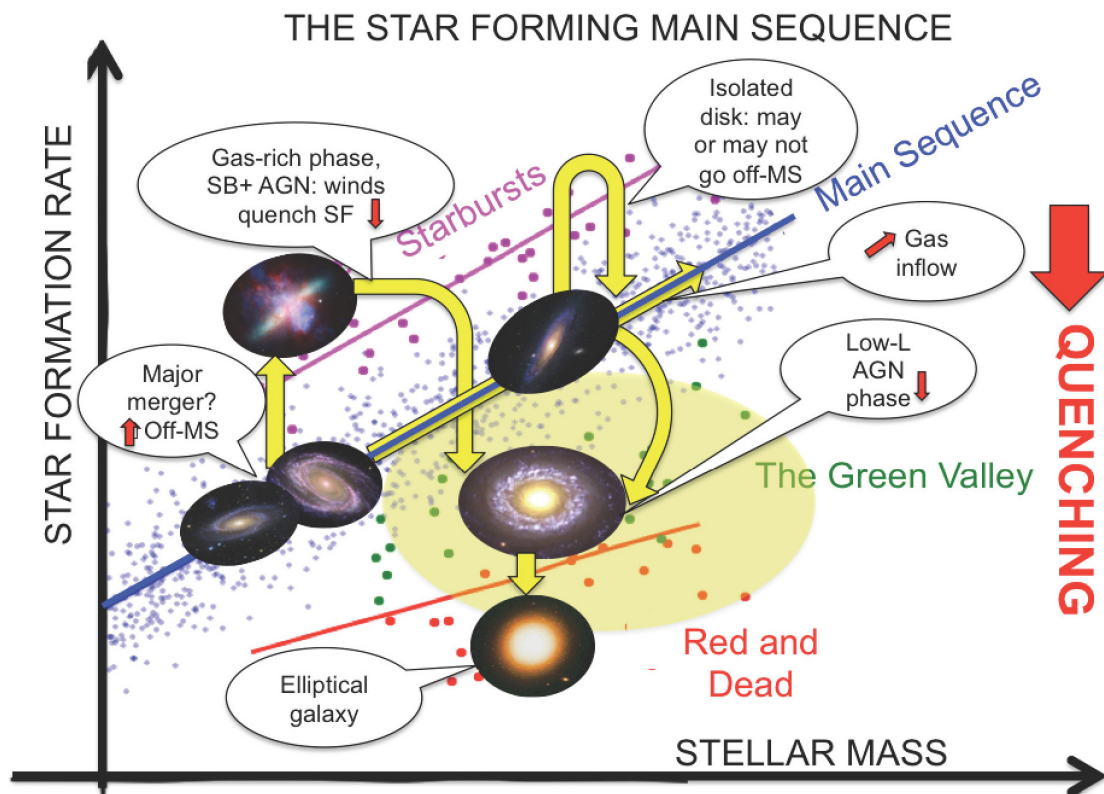


Figure 3.1: Summary of the episodes that a source could experience along the (SFR, M_*) . Courtesy of C.Gruppioni

Although the discussion of the characteristics of the other two populations present in the plane (SFR, M_*) is beyond the scope of this thesis, it is clear that they may have some evolutionary connection with the “normal” star-forming galaxies that populate the MS. This is one of the main features shown in fig. 3.1. In this picture, galaxies evolve along the MS, their star formation being fuelled by continuous flows of cold gas from the cosmic web (gas inflows). However, some events could bring them off-MS in the starburst or passive (i.e., red and dead) regions. For instance, it has been proposed that a major merger could produce an enhancement of star formation, bringing galaxies up to the starburst locus. On the other hand, a star-forming (normal or starburst) galaxy could rapidly exhaust its gas, due to strong AGN feedback, or other processes, then falling

into the passive galaxy region. Further studies are needed to test these interpretations, and in particular to understand the nature of starburst galaxies and their link with the other two populations. Another important point to clarify is the role of AGNs in the exhaustion of gas within their hosts. Finally, the environment in which galaxies form and evolve can contribute to feed or deplete gas into/from the galaxy, therefore affecting the star formation within. Hence, studies of galaxy clusters are also crucial to understand how the intergalactic and interstellar medium affect the evolution of a Galaxy.

List of Figures

1.1	The Hubble sequence of galaxies	3
1.2	Overview of the stellar population synthesis technique	6
1.3	SED fitting example	8
1.4	SED fitting example	8
2.1	Three dimensional Main sequence for SDSS galaxies at $0.02 < z < 0.085$. .	12
2.2	Main sequence of Star forming galaxies. Best fits from different studies . .	13
2.3	Main sequence of star forming galaxies from three redshifts. CANDELS samples at $z = 4, 5$ & 6	13
2.4	Comparison of SFR from UV and IR for the same sample on a fitted MS of SFG	15
2.5	Evolution of MS of SFG with redshift	16
2.6	Evolution of the Specific star formation with redshift	17
2.7	Mean Specific star formation rate vs redshift for various Mass bins	18
2.8	Variation of de specific star formation rate with mass at different redshifts	18
2.9	Contribution of off-sequence galaxies to the total SFR density in different SFR bins	20
3.1	Cartoon:Main sequence of Star Forming Galaxies possible evolution tracks	22

Bibliography

- Allen, C. W. (1976). *Astrophysical Quantities*. London: Athlone (3rd edition).
- Ashby, M. L. N., Willner, S. P., Fazio, G. G., Huang, J.-S., Arendt, R., Barmby, P., Barro, G., Bell, E. F., Bouwens, R., Cattaneo, A., Croton, D., Davé, R., Dunlop, J. S., Egami, E., Faber, S., Finlator, K., Grogin, N. A., Guhathakurta, P., Hernquist, L., Hora, J. L., Illingworth, G., Kashlinsky, A., Koekemoer, A. M., Koo, D. C., Labbé, I., Li, Y., Lin, L., Moseley, H., Nandra, K., Newman, J., Noeske, K., Ouchi, M., Peth, M., Rigopoulou, D., Robertson, B., Sarajedini, V., Simard, L., Smith, H. A., Wang, Z., Wechsler, R., Weiner, B., Wilson, G., Wuyts, S., Yamada, T., and Yan, H. (2013). SEDS: The Spitzer Extended Deep Survey. Survey Design, Photometry, and Deep IRAC Source Counts. *Astrophysical Journal*, 769:80.
- Bauer, A. E., Conselice, C. J., Pérez-González, P. G., Grützbauch, R., Bluck, A. F. L., Buitrago, F., and Mortlock, A. (2011). Star formation in a stellar mass-selected sample of galaxies to $z = 3$ from the GOODS-NICMOS Survey. *Monthly Notices of the Royal Astronomical Society*, 417:289–303.
- Brinchmann, J., Charlot, S., White, S. D. M., Tremonti, C., Kauffmann, G., Heckman, T., and Brinkmann, J. (2004). The physical properties of star-forming galaxies in the low-redshift Universe. *Monthly Notices of the Royal Astronomical Society*, 351:1151–1179.
- Calzetti, D., Armus, L., Bohlin, R. C., Kinney, A. L., Koornneef, J., and Storchi-Bergmann, T. (2000). The Dust Content and Opacity of Actively Star-forming Galaxies. *Astrophysical Journal*, 533:682–695.
- Chabrier, G. (2003). Galactic Stellar and Substellar Initial Mass Function. *Publications of the Astronomical Society of the Pacific*, 115:763–795.
- Conroy, C. (2013). Modeling the Panchromatic Spectral Energy Distributions of Galaxies. *Annual Review of Astronomy and Astrophysics*, 51:393–455.
- Cowie, L. L., Songaila, A., Hu, E. M., and Cohen, J. G. (1996). New Insight on Galaxy Formation and Evolution From Keck Spectroscopy of the Hawaii Deep Fields. *Astronomical Journal*, 112:839.
- Daddi, E., Dickinson, M., Morrison, G., Chary, R., Cimatti, A., Elbaz, D., Frayer, D., Renzini, A., Pope, A., Alexander, D. M., Bauer, F. E., Giavalisco, M., Huynh, M., Kurk, J., and Mignoli, M. (2007). Multiwavelength Study of Massive Galaxies at $z \sim 2$. I. Star Formation and Galaxy Growth. *Astrophysical Journal, Letters*, 670:156–172.

- Davis, M., Guhathakurta, P., Konidakis, N. P., Newman, J. A., Ashby, M. L. N., Biggs, A. D., Barmby, P., Bundy, K., Chapman, S. C., Coil, A. L., Conselice, C. J., Cooper, M. C., Croton, D. J., Eisenhardt, P. R. M., Ellis, R. S., Faber, S. M., Fang, T., Fazio, G. G., Georgakakis, A., Gerke, B. F., Goss, W. M., Gwyn, S., Harker, J., Hopkins, A. M., Huang, J.-S., Ivison, R. J., Kassin, S. A., Kirby, E. N., Koekemoer, A. M., Koo, D. C., Laird, E. S., Le Floch, E., Lin, L., Lotz, J. M., Marshall, P. J., Martin, D. C., Metevier, A. J., Moustakas, L. A., Nandra, K., Noeske, K. G., Papovich, C., Phillips, A. C., Rich, R. M., Rieke, G. H., Rigopoulou, D., Salim, S., Schiminovich, D., Simard, L., Smail, I., Small, T. A., Weiner, B. J., Willmer, C. N. A., Willner, S. P., Wilson, G., Wright, E. L., and Yan, R. (2007). The All-Wavelength Extended Groth Strip International Survey (AEGIS) Data Sets. *Astrophysical Journal, Letters*, 660:L1–L6.
- Eales, S., de Vis, P., Smith, M. W. L., Appah, K., Ciesla, L., Duffield, C., and Schofield, S. (2017). The Galaxy End Sequence. *Monthly Notices of the Royal Astronomical Society*, 465:3125–3133.
- Eales, S., Smith, D., Bourne, N., Loveday, J., Rowlands, K., van der Werf, P., Driver, S., Dunne, L., Dye, S., Furlanetto, C., Ivison, R. J., Maddox, S., Robotham, A., Smith, M. W. L., Taylor, E. N., Valiante, E., Wright, A., Cigan, P., De Zotti, G., Jarvis, M. J., Marchetti, L., Michałowski, M. J., Phillipps, S., Viaene, S., and Vlahakis, C. (2018). The new galaxy evolution paradigm revealed by the Herschel surveys. *Monthly Notices of the Royal Astronomical Society*, 473:3507–3524.
- Elbaz, D., Daddi, E., Le Borgne, D., Dickinson, M., Alexander, D. M., Chary, R.-R., Starck, J.-L., Brandt, W. N., Kitzbichler, M., MacDonald, E., Nonino, M., Popesso, P., Stern, D., and Vanzella, E. (2007). The reversal of the star formation-density relation in the distant universe. *Astronomy and Astrophysics*, 468:33–48.
- Feldmann, R. (2017). Are star formation rates of galaxies bimodal? *Monthly Notices of the Royal Astronomical Society*, 470:L59–L63.
- Fitzpatrick, E. L. (1986). An average interstellar extinction curve for the Large Magellanic Cloud. *Astronomical Journal*, 92:1068–1073.
- Guo, K., Zheng, X. Z., and Fu, H. (2013). The Intrinsic Scatter along the Main Sequence of Star-forming Galaxies at $z \sim 0.7$. *Astrophysical Journal*, 778:23.
- Hubble, E. P. (1936). *Realm of the Nebulae*. New Haven: Yale University Press.
- Ilbert, O., Arnouts, S., Le Floch, E., Aussel, H., Bethermin, M., Capak, P., Hsieh, B.-C., Kajisawa, M., Karim, A., Le Fèvre, O., Lee, N., Lilly, S., McCracken, H. J., Michel-Dansac, L., Moutard, T., Renzini, M. A., Salvato, M., Sanders, D. B., Scoville, N., Sheth, K., Silverman, J. D., Smolčić, V., Taniguchi, Y., and Tresse, L. (2015). Evolution of the specific star formation rate function at $z < 1.4$ Dissecting the mass-SFR plane in COSMOS and GOODS. *Astronomy and Astrophysics*, 579:A2.
- Karim, A., Schinnerer, E., Martínez-Sansigre, A., Sargent, M. T., van der Wel, A., Rix, H.-W., Ilbert, O., Smolčić, V., Carilli, C., Pannella, M., Koekemoer, A. M., Bell, E. F., and Salvato, M. (2011). The Star Formation History of Mass-selected Galaxies in the COSMOS Field. *Astrophysical Journal*, 730:61.

- Kennicutt, Jr., R. C. (1998). Star Formation in Galaxies Along the Hubble Sequence. *Annual Review of Astronomy and Astrophysics*, 36:189–232.
- Kennicutt, Jr., R. C., Hao, C.-N., Calzetti, D., Moustakas, J., Dale, D. A., Bendo, G., Engelbracht, C. W., Johnson, B. D., and Lee, J. C. (2009). Dust-corrected Star Formation Rates of Galaxies. I. Combinations of H α and Infrared Tracers. *Astrophysical Journal*, 703:1672–1695.
- Kroupa, P. (2001). On the variation of the initial mass function. *Monthly Notices of the Royal Astronomical Society*, 322:231–246.
- Laigle, C., McCracken, H. J., Ilbert, O., Hsieh, B. C., Davidzon, I., Capak, P., Hasinger, G., Silverman, J. D., Pichon, C., Coupon, J., Aussel, H., Le Borgne, D., Caputi, K., Cassata, P., Chang, Y.-Y., Civano, F., Dunlop, J., Fynbo, J., Kartaltepe, J. S., Koekemoer, A., Le Fèvre, O., Le Floch, E., Leauthaud, A., Lilly, S., Lin, L., Marchesi, S., Milvang-Jensen, B., Salvato, M., Sanders, D. B., Scoville, N., Smolcic, V., Stockmann, M., Taniguchi, Y., Tasca, L., Toft, S., Vaccari, M., and Zabl, J. (2016). The COSMOS2015 Catalog: Exploring the $1 < z < 6$ Universe with Half a Million Galaxies. *Astrophysical Journal*, 224:24.
- Lee, N., Sanders, D. B., Casey, C. M., Toft, S., Scoville, N. Z., Hung, C.-L., Floch, E. L., Ilbert, O., Zahid, H. J., Aussel, H., Capak, P., Kartaltepe, J. S., Kewley, L. J., Li, Y., Schawinski, K., Sheth, K., and Xiao, Q. (2015). A turnover in the galaxy main sequence of star formation at $M_* \sim 10^{10} M_\odot$ for redshifts $z < 1.3$. *Astrophysical Journal*, 801(2):80.
- Madau, P. and Dickinson, M. (2014). Cosmic Star-Formation History. *Annual Review of Astronomy and Astrophysics*, 52:415–486.
- Maraston, C., Pforr, J., Henriques, B. M., Thomas, D., Wake, D., Brownstein, J. R., Capozzi, D., Tinker, J., Bundy, K., Skibba, R. A., Beifiori, A., Nichol, R. C., Edmondson, E., Schneider, D. P., Chen, Y., Masters, K. L., Steele, O., Bolton, A. S., York, D. G., Weaver, B. A., Higgs, T., Bizyaev, D., Brewington, H., Malanushenko, E., Malanushenko, V., Snedden, S., Oravetz, D., Pan, K., Shelden, A., and Simmons, A. (2013). Stellar masses of SDSS-III/BOSS galaxies at $z \sim 0.5$ and constraints to galaxy formation models. *Monthly Notices of the Royal Astronomical Society*, 435:2764–2792.
- Mobasher, B., Dahlen, T., Ferguson, H. C., Acquaviva, V., Barro, G., Finkelstein, S. L., Fontana, A., Gruetzbauch, R., Johnson, S., Lu, Y., Papovich, C. J., Pforr, J., Salvato, M., Somerville, R. S., Wiklind, T., Wuyts, S., Ashby, M. L. N., Bell, E., Conselice, C. J., Dickinson, M. E., Faber, S. M., Fazio, G., Finlator, K., Galametz, A., Gawiser, E., Giavalisco, M., Grazian, A., Grogin, N. A., Guo, Y., Hathi, N., Kocevski, D., Koekemoer, A. M., Koo, D. C., Newman, J. A., Reddy, N., Santini, P., and Wechsler, R. H. (2015). A Critical Assessment of Stellar Mass Measurement Methods. *Astrophysical Journal*, 808:101.
- Noeske, K. G., Faber, S. M., Weiner, B. J., Koo, D. C., Primack, J. R., Dekel, A., Papovich, C., Conselice, C. J., Le Floch, E., Rieke, G. H., Coil, A. L., Lotz, J. M., Somerville, R. S., and Bundy, K. (2007a). Star Formation in AEGIS Field Galaxies since $z=1.1$: Staged Galaxy Formation and a Model of Mass-dependent Gas Exhaustion. *Astrophysical Journal, Letters*, 660:L47–L50.

- Noeske, K. G., Weiner, B. J., Faber, S. M., Papovich, C., Koo, D. C., Somerville, R. S., Bundy, K., Conselice, C. J., Newman, J. A., Schiminovich, D., Le Floch, E., Coil, A. L., Rieke, G. H., Lotz, J. M., Primack, J. R., Barmby, P., Cooper, M. C., Davis, M., Ellis, R. S., Fazio, G. G., Guhathakurta, P., Huang, J., Kassin, S. A., Martin, D. C., Phillips, A. C., Rich, R. M., Small, T. A., Willmer, C. N. A., and Wilson, G. (2007b). Star Formation in AEGIS Field Galaxies since $z=1.1$: The Dominance of Gradually Declining Star Formation, and the Main Sequence of Star-forming Galaxies. *Astrophysical Journal, Letters*, 660:L43–L46.
- Pannella, M., Carilli, C. L., Daddi, E., McCracken, H. J., Owen, F. N., Renzini, A., Strazzullo, V., Civano, F., Koekemoer, A. M., Schinnerer, E., Scoville, N., Smolčić, V., Taniguchi, Y., Aussel, H., Kneib, J. P., Ilbert, O., Mellier, Y., Salvato, M., Thompson, D., and Willott, C. J. (2009). Star Formation and Dust Obscuration at $z \approx 2$: Galaxies at the Dawn of Downsizing. *Astrophysical Journal, Letters*, 698:L116–L120.
- Pérez-González, P. G., Trujillo, I., Barro, G., Gallego, J., Zamorano, J., and Conselice, C. J. (2008). Exploring the Evolutionary Paths of the Most Massive Galaxies since $z \sim 2$. *Astrophysical Journal*, 687:50–58.
- Prevot, M. L., Lequeux, J., Prevot, L., Maurice, E., and Rocca-Volmerange, B. (1984). The typical interstellar extinction in the Small Magellanic Cloud. *Astronomy and Astrophysics*, 132:389–392.
- Renzini, A. and Peng, Y.-j. (2015). An Objective Definition for the Main Sequence of Star-forming Galaxies. *Astrophysical Journal, Letters*, 801:L29.
- Rodighiero, G., Cimatti, A., Gruppioni, C., Popesso, P., Andreani, P., Altieri, B., Aussel, H., Berta, S., Bongiovanni, A., Brisbin, D., Cava, A., Cepa, J., Daddi, E., Dominguez-Sanchez, H., Elbaz, D., Fontana, A., Förster Schreiber, N., Franceschini, A., Genzel, R., Grazian, A., Lutz, D., Magdis, G., Magliocchetti, M., Magnelli, B., Maiolino, R., Mancini, C., Nordon, R., Perez Garcia, A. M., Poglitsch, A., Santini, P., Sanchez-Portal, M., Pozzi, F., Riguccini, L., Saintonge, A., Shao, L., Sturm, E., Tacconi, L., Valtchanov, I., Wetzstein, M., and Wieprecht, E. (2010). The first Herschel view of the mass-SFR link in high- z galaxies. *Astronomy and Astrophysics*, 518:L25.
- Rodighiero, G., Daddi, E., Baronchelli, I., Cimatti, A., Renzini, A., Aussel, H., Popesso, P., Lutz, D., Andreani, P., Berta, S., Cava, A., Elbaz, D., Feltre, A., Fontana, A., Schreiber, N. M. F., Franceschini, A., Genzel, R., Grazian, A., Gruppioni, C., Ilbert, O., Floch, E. L., Magdis, G., Magliocchetti, M., Magnelli, B., Maiolino, R., McCracken, H., Nordon, R., Poglitsch, A., Santini, P., Pozzi, F., Riguccini, L., Tacconi, L. J., Wuyts, S., and Zamorani, G. (2011). The lesser role of starbursts in star formation at $z = 2$. *Astrophysical Journal, Letters*, 739(2):L40.
- Rodighiero, G., Renzini, A., Daddi, E., Baronchelli, I., Berta, S., Cresci, G., Franceschini, A., Gruppioni, C., Lutz, D., Mancini, C., Santini, P., Zamorani, G., Silverman, J., Kashino, D., Andreani, P., Cimatti, A., Sánchez, H. D., Le Floch, E., Magnelli, B., Popesso, P., and Pozzi, F. (2014). A multiwavelength consensus on the main sequence of star-forming galaxies at $z \sim 2$. *Monthly Notices of the Royal Astronomical Society*, 443:19–30.

- Salmon, B., Papovich, C., Finkelstein, S. L., Tilvi, V., Finlator, K., Behroozi, P., Dahlen, T., Davé, R., Dekel, A., Dickinson, M., Ferguson, H. C., Giavalisco, M., Long, J., Lu, Y., Mobasher, B., Reddy, N., Somerville, R. S., and Wechsler, R. H. (2015). The Relation between Star Formation Rate and Stellar Mass for Galaxies at $3.5 \leq z \leq 6.5$ in CANDELS. *Astrophysical Journal*, 799:183.
- Salpeter, E. E. (1955). The Luminosity Function and Stellar Evolution. *Astrophysical Journal*, 121:161.
- Santini, P., Ferguson, H. C., Fontana, A., Mobasher, B., Barro, G., Castellano, M., Finkelstein, S. L., Grazian, A., Hsu, L. T., Lee, B., Lee, S.-K., Pforr, J., Salvato, M., Wiklind, T., Wuyts, S., Almaini, O., Cooper, M. C., Galametz, A., Weiner, B., Amorin, R., Boutsia, K., Conselice, C. J., Dahlen, T., Dickinson, M. E., Giavalisco, M., Grogin, N. A., Guo, Y., Hathi, N. P., Kocevski, D., Koekemoer, A. M., Kurczynski, P., Merlin, E., Mortlock, A., Newman, J. A., Paris, D., Pentericci, L., Simons, R., and Willner, S. P. (2015). Stellar masses from the candels survey: The goods-south and uds fields. *Astrophysical Journal*, 801(2):97.
- Sargent, M. T., Daddi, E., Béthermin, M., Aussel, H., Magdis, G., Hwang, H. S., Juneau, S., Elbaz, D., and da Cunha, E. (2014). Regularity Underlying Complexity: A Redshift-independent Description of the Continuous Variation of Galaxy-scale Molecular Gas Properties in the Mass-star Formation Rate Plane. *Astrophysical Journal*, 793:19.
- Schreiber, C., Pannella, M., Elbaz, D., Béthermin, M., Inami, H., Dickinson, M., Magnelli, B., Wang, T., Aussel, H., Daddi, E., Juneau, S., Shu, X., Sargent, M. T., Buat, V., Faber, S. M., Ferguson, H. C., Giavalisco, M., Koekemoer, A. M., Magdis, G., Morrison, G. E., Papovich, C., Santini, P., and Scott, D. (2015). The Herschel view of the dominant mode of galaxy growth from $z = 4$ to the present day. *Astronomy and Astrophysics*, 575:A74.
- Seaton, M. J. (1979). Interstellar extinction in the UV. *Monthly Notices of the Royal Astronomical Society*, 187:73P–76P.
- Speagle, J. S., Steinhardt, C. L., Capak, P. L., and Silverman, J. D. (2014). A Highly Consistent Framework for the Evolution of the Star-Forming “Main Sequence” from $z \sim 0$ to $z \sim 6$. *Astrophysical Journal, Supplement*, 214:15.
- Whitaker, K. E., van Dokkum, P. G., Brammer, G., and Franx, M. (2012). The Star Formation Mass Sequence Out to $z = 2.5$. *Astrophysical Journal*, 754:L29.
- York, D. G., Adelman, J., Anderson, Jr., J. E., Anderson, S. F., Annis, J., Bahcall, N. A., Bakken, J. A., Barkhouser, R., Bastian, S., Berman, E., Boroski, W. N., Bracker, S., Briegel, C., Briggs, J. W., Brinkmann, J., Brunner, R., Burles, S., Carey, L., Carr, M. A., Castander, F. J., Chen, B., Colestock, P. L., Connolly, A. J., Crocker, J. H., Csabai, I., Czarapata, P. C., Davis, J. E., Doi, M., Dombeck, T., Eisenstein, D., Ellman, N., Elms, B. R., Evans, M. L., Fan, X., Federwitz, G. R., Fiscelli, L., Friedman, S., Frieman, J. A., Fukugita, M., Gillespie, B., Gunn, J. E., Gurbani, V. K., de Haas, E., Haldeman, M., Harris, F. H., Hayes, J., Heckman, T. M., Hennessy, G. S., Hindsley, R. B., Holm, S., Holmgren, D. J., Huang, C.-h., Hull, C., Husby, D., Ichikawa, S.-I., Ichikawa, T., Ivezić, Ž., Kent, S., Kim, R. S. J., Kinney, E., Klaene, M., Kleinman,

A. N., Kleinman, S., Knapp, G. R., Korienek, J., Kron, R. G., Kunszt, P. Z., Lamb, D. Q., Lee, B., Leger, R. F., Limmongkol, S., Lindenmeyer, C., Long, D. C., Loomis, C., Loveday, J., Lucinio, R., Lupton, R. H., MacKinnon, B., Mannery, E. J., Mantsch, P. M., Margon, B., McGehee, P., McKay, T. A., Meiksin, A., Merelli, A., Monet, D. G., Munn, J. A., Narayanan, V. K., Nash, T., Neilsen, E., Neswold, R., Newberg, H. J., Nichol, R. C., Nicinski, T., Nonino, M., Okada, N., Okamura, S., Ostriker, J. P., Owen, R., Pauls, A. G., Peoples, J., Peterson, R. L., Petravick, D., Pier, J. R., Pope, A., Pordes, R., Prosapio, A., Rechenmacher, R., Quinn, T. R., Richards, G. T., Richmond, M. W., Rivetta, C. H., Rockosi, C. M., Ruthmansdorfer, K., Sandford, D., Schlegel, D. J., Schneider, D. P., Sekiguchi, M., Sergey, G., Shimasaku, K., Siegmund, W. A., Smee, S., Smith, J. A., Snedden, S., Stone, R., Stoughton, C., Strauss, M. A., Stubbs, C., SubbaRao, M., Szalay, A. S., Szapudi, I., Szokoly, G. P., Thakar, A. R., Tremonti, C., Tucker, D. L., Uomoto, A., Vanden Berk, D., Vogeley, M. S., Waddell, P., Wang, S.-i., Watanabe, M., Weinberg, D. H., Yanny, B., Yasuda, N., and SDSS Collaboration (2000). The Sloan Digital Sky Survey: Technical Summary. *Astronomical Journal*, 120:1579–1587.